Iberdrola Innovation Middle East

26/08/2021

Distributed ReStart: Non-conventional Black-Start Resources

Tx Energization & Grid Forming Converters Control for Black-Start Applications

IBERDROLA

GENERAL NOTES

Customer Details	
Customer	SP Energy Networks
Address	320 St. Vincent Street, Glasgow, G2 5AD
Contact	Neil.Miller@spenergynetworks.co.uk cfoote@spenergynetworks.co.uk
Reference	Neil Miller, Colin Foote

Iberdrola Innovation Middle East	
Legal Entity	Iberdrola QSTP LLC
Address	Qatar Science & Technology Park Tech 1 Building, Office 204, Doha Qatar PO Box 210177
Document Author	Abdulrahman Alassi (aalassi@iberdrola.com)

About this Document	
Title	Distributed ReStart: Tx Energization and GFC Control for Black-Start Applications
Date of Issue	26/08/2021
Version	1.1
Internal Reference	20R11

REVISION CONTROL

REV	DATE	REASON
0.1	14/03/2021	Document creation
0.2	24/05/2021	Post SPEN Feedback Update
1.0	24/06/2021	Document Update & Review
1.1	26/08/2021	Published Version Review

CONTENTS

Executive Summary

This report presents the outcomes of WP 2 from the collaboration project between Iberdrola Innovation Middle East and Scottish Power Energy Networks in relation to Distributed ReStart. The report investigates the use of converter-based generation in black start applications. The presented results are focused in two main parts: a) transformer energization; b) virtual synchronous machine (VSM) grid forming control for a simplified network black start scenario.

Comprehensive transformer energization analysis and simulations are presented for single and three phase transformers with different configurations, with the aim of assessing the available energization techniques that mitigate the risk of the transformer inrush current on the converter used for energization. The assessment covers hard, controlled, and soft transformer energizations, with theoretical background and simulated tests.

Controlled energization of independent phase breakers can eliminate inrush current when closed at optimal instants. The availability of phase independent breakers may be limited in some networks. Soft transformer energization through grid-forming converters can thus be considered as an effective inrush current mitigation technique.

The VSM grid-forming control is modified to reflect key black-start requirements such as ramping voltage control at the connection point with load pickup, as well as grid synchronization. Different load pickup scenarios are covered in the report to assess the variation between simultaneous and sequential load energization from the grid-forming converter.

The results show satisfactory performance for the modified VSM control in achieving the test targets while maintaining converter power, frequency, and current control limits within normal operating boundaries. Future tests are planned to investigate the inrush current mitigation and VSM control performance for larger network segments energization.

1. Introduction

The emerging new power systems paradigm with increasing distributed energy resources (DER) is mandating changes to the way traditional electricity services are provided. The first deliverable of this study was published in Chapter 10 of the "Power Engineering and Trials - Power Systems Studies Part 1" report. That chapter shed light on the increasing role of converters-based generation to participate in ancillary services provision, such as black start, and highlighted the relevant challenges such as transformers inrush current mitigation and frequency stability at a high level, in addition to comparing the performance of four grid-forming control techniques with black start capabilities.

This report builds on the previous study and provides more insights on the grid-forming converter control based on a modified virtual synchronous machine (VSM) structure for black-start. Also, given the instrumental role of smooth transformer energization during black start, a detailed investigation is first carried out to study and outline the different energization techniques and their suitability for the application based on ideal energizing voltage source assumption, such as: hard energization, controlled (point-on-wave) and soft energization.

Different operating modes for the grid-forming VSM control are tested through load blocks pick up at the point of common coupling (PCC), voltage control and finally grid synchronization after black-start. The high-level network model that is used as a basis for grid-forming converters control analysis in the second part of this report is presented in Figure 1.

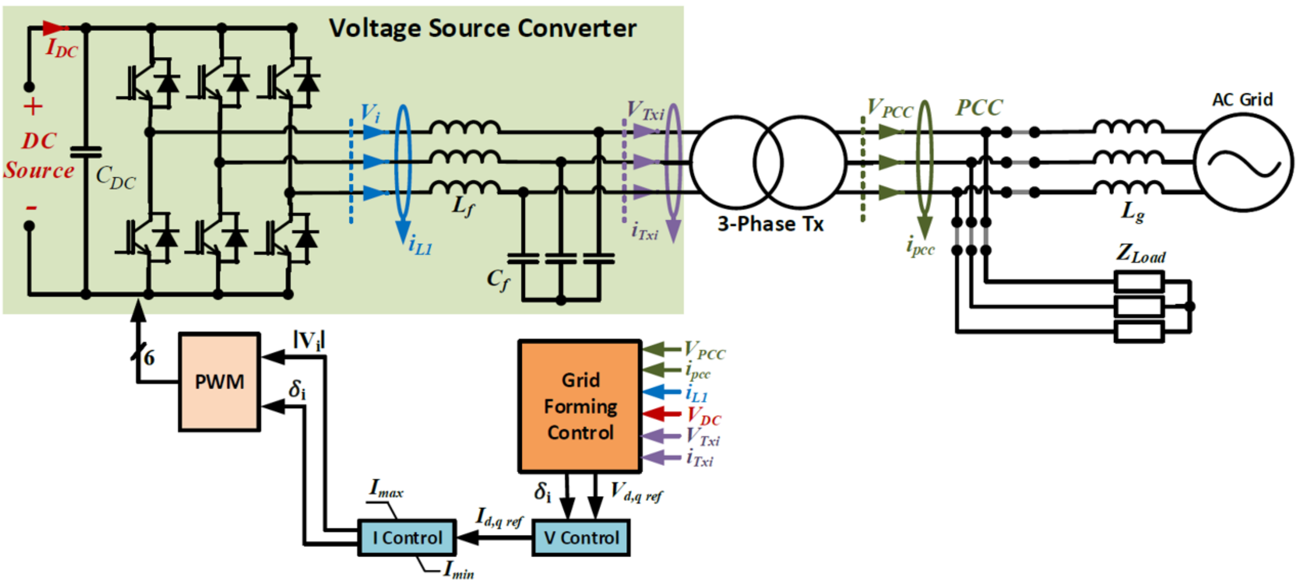

Figure 1: High level block diagram of the network used for grid-forming control analysis in this report.

The rest of the report is structured as follows: Section 2 presents background overview on transformer energization techniques. Section 3 then presents comprehensive simulation analysis for transformer energization in single and three phase configurations to visualize the performance of each technique under common test conditions. Then, a complete black-start scenario is presented in Section 4 based on the network in Figure 1. The distribution transformer is first energized with soft energization, and then various load pickup scenarios are covered, followed by grid synchronization. Finally, the report is summarized in Section 5.

2. Transformers Energization

Transformers inrush current mitigation has traditionally been considered to address some protection and reliability concerns but in most cases the sources used were capable of delivering the required high inrush currents for short times. Nowadays, this issue becomes more challenging for the case of converter-based sources that do not have the same current overload capability.

The main challenge in transformers re-energization arises from the transformer core non-linearity and saturation behavior. Typically, transformers are designed to operate in the linear region of the flux (ϕ) and magnetizing current (i_M) curve near the knee of the curve (i.e., with a slightly varying high magnetizing branch inductance). Figure 2 illustrates a single-phase electrical model of a transformer (R_1, L_1, R_2 and L_2 are the primary and secondary windings resistance and inductance, respectively, and R_m and L_{sat} are the core resistance and inductance, respectively). When the core is saturated, the effective core inductance L_{sat} value is severely reduced, which draws significantly higher current to the transformer core due to the reduced equivalent impedance (even when the secondary side is left open).

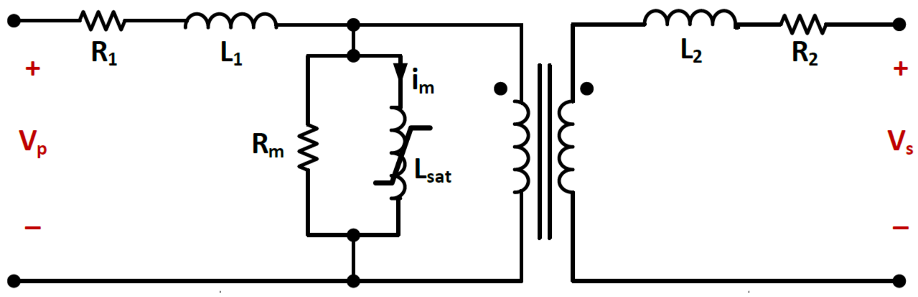

Figure 2: Electrical model for a single-phase transformer.

Two methods are conventionally used to illustrate and model this phenomenon. First, through hysteresis loops (more realistic), and the second through approximated piecewise linear segments to represent the ϕ $vs.$ i_M curve (widely used approximation that preserves key saturation trends with reduced complexity). Figure 3 illustrates the two approximations, where ϕ_r is the residual flux and ϕ_{sat} is the saturation flux.

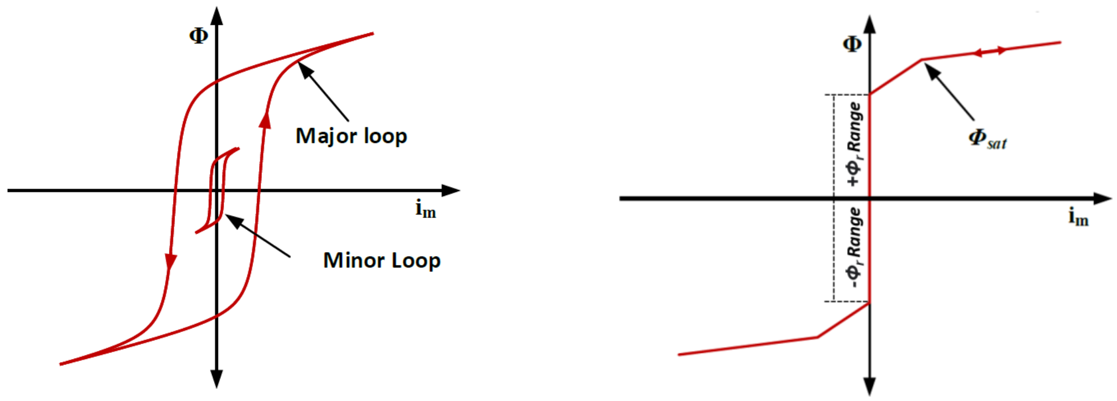

(a) (b)

Figure 3: Transformer core magnetizing curve: (a) hysteresis loops, (b) piecewise linear segments.

When a transformer is de-energized, the core flux does not necessarily decay to zero when the magnetizing current is zero, which is due to the core magnetization properties. The magnitude of this residual flux ϕ_r depends on the instant of de-energization since flux is generally defined as the core voltage integral and thus similarly follows a sinusoid steady state waveform. Consequently, if a transformer is re-energized by randomly closing the circuit breaker switch, then there exists a possibility (depending on the energizing instant) for the flux to have a maximum value of $\phi_r + 2\phi_m$ if the transformer is connected at the voltage waveform zero-crossing, where ϕ_m is the nominal maximum flux value. Figure 4 illustrates a comparison between: a) normal operating condition where a transformer flux oscillates between -1 and 1 pu, and the reflection of that on inrush current (minimal value), and b) saturated condition that shifts the flux curve and causes a corresponding increase in the core magnetizing into saturation, causing inrush current.

Mathematical models can be used to analyze transformer core saturation and mitigation techniques and understand their operation. Different electric and magnetic circuit models and simulation tools are presented in literature for this task, with the transformer configuration dictating the model complexity. For instance, three phase transformers with a single core are modeled with additional inductive core branch to link the different phases due to the former flux inter-phase interactions. Collectively, the mathematical model presented here is for a single-phase transformer, and is then generalized to three-phase units while taking relevant variations into account through simulation results in section 3.

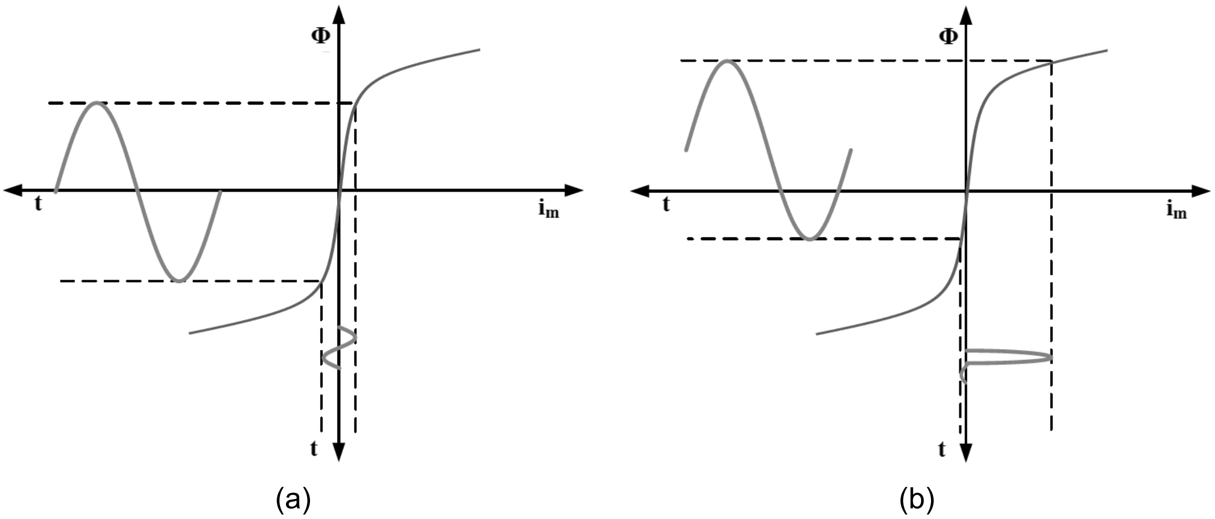

Figure 4: generic transformer saturation curve: (a) normal operation, (b) saturated core in the positive direction.

2.1. Transformer energization techniques

Several methods to mitigate inrush current during transformer energization are investigated and proposed in literature, ranging from random/manual energization with or without current limiting resistors, to optimization/control based techniques. Mathematically, the instantaneous core flux value in single-phase transformers relies on several factors such as voltage magnitude, energizing phase angle, residual flux and circuit impedance parameters. Equation (1) presents a theoretical flux calculation based on a simplified version of the primary side circuit in Figure 2.

$$\phi \approx \frac{-LV_p\cos(\omega t+\alpha)}{\sqrt{R_1^2+(\omega L)^2}} + \left(\phi_r + \frac{LV_p\cos(\alpha)}{\sqrt{R_1^2+(\omega L)^2}}\right)e^{-\frac{R_1}{L}t} \quad (1)$$

where V_p is the primary source voltage, ω is the source angular frequency, R_1 is the primary windings resistance, L is the average energized winding inductance, and α is the energization instant on the voltage waveform.

The simplified circuit model in equation (1) assumes that R_m is significantly higher than the impedance of L_{sat} in Figure 2. Such simplification helps reducing the circuit analysis complexity with neat mathematical expressions as a first approximation that investigates key parameters impact. From equation (1), the flux equation consists of two terms, a steady state and a transient one. The latter decays with a time constant related to the RL values and is mainly responsible for the inrush current.

Hard Transformer Energization

The simplest method to start a transformer is to randomly connect it to a 1 pu voltage source. However, in this case, it is unknown what the angle-shift value (α) is (the initial point on voltage waveform). In the worst-case scenario when $\alpha = 0$ and $t = 0$, the flux value theoretically approaches $2\phi_m + \phi_r$, producing the highest inrush current at the first peak. The random starting technique is termed “Hard-energization”. It is noteworthy that for a three-phase transformer, closing the breaker based on the optimal instant for one of the phases based on equation (1) can still produce inrush current in the other phases.

Hard Energization with Pre-Insertion Resistors (PIR)

A well-established technique is to insert a series resistor (pre-insertion resistor, PIR) between the energizing source and the transformer to mitigate inrush current. This is effectively represented in equation (1) through adding the PIR value to that of R_1 in series. This way, the flux saturation magnitude is mitigated, and its exponential term decay is accelerated through modifying the RL circuit decay time constant. Bypass switches and thermal resistors have also been proposed to achieve this task. Thermal resistors have minimal impedance under normal operating condition but exhibit higher current limiting capability under higher temperature (i.e., inrush current) conditions. A recent proposal suggested the use of superconducting fault current limiters (SFCL) for this task.

Controlled Switching Transformer Energization

On the other hand, optimized operation techniques have been increasingly used to eliminate inrush currents in single and three phase transformers. The first technique is termed “controlled-switching” or “point-on-wave switching” and can be directly explained from equation (1). That is, if switching takes place at an optimal angle α when the residual flux is equal to the ‘prospective flux’, then the inrush current in the respective phase is theoretically eliminated. Prospective flux is defined as the source voltage integral at the breaker input. In this case, the residual flux impact is neutralized and what remains is merely the sinusoid steady-state part of the equation.

This technique requires prior knowledge of the residual flux ϕ_r such that the switching angle α can be tuned accordingly. Flux can be estimated by measuring the primary core voltage integral, and the residual flux value is then recorded as the steady-state flux value following transformer de-energization. Figure 5 illustrates the optimal switching instant for a single-phase transformer example. The switching here takes place when the residual flux is equal to the prospective flux, and then both waveforms continue in synchronism. Controlled transformer energization is independent of converter control and requires independent/ fast control of circuit breaker phases to avoid breaker delays.

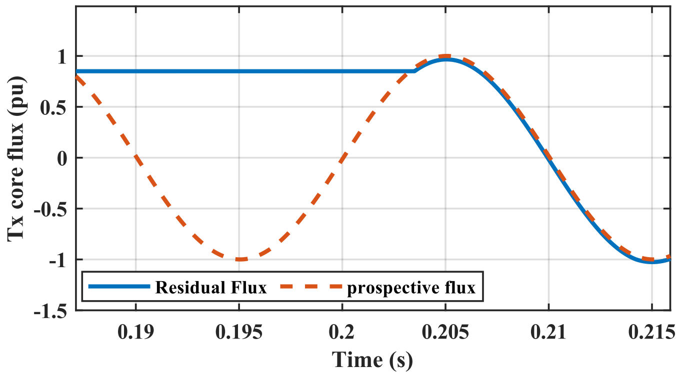

Figure 5: Prospective and core flux illustration in a single-phase transformer.

Soft Transformer Energization

A different transformer energizing technique is to supply a voltage ramp from zero to 1 pu between $t = \mathrm{t}_0$ *and* $t = \mathrm{t}_0 + T_{ramp}$ to the transformer primary windings rather than a full instantaneous voltage at $t = \mathrm{t}_0$ as the case for the previous techniques. In this case, two opposing trends act against each other: a) the exponential decay of the transient, and b) the voltage build up from the ramp.

The flux starts from its residual value ϕ_r, and the ramping time should be selected in such a way that balances these two opposing actions. That is, if a short ramping time is considered, then the voltage will build up much faster than the transient exponential decay and the core can still be saturated, and a high inrush current is produced. Instead, the ramping time should be selected so that the voltage builds up is slow enough to allow for the transient to decay first without saturating the core. Figure 6 illustrates an example for the ramping voltage concept used in soft energization. In Figure 6b, the flux-magnetizing current curve initiates from the residual flux point on the y-axis, and spirals slowly all the way to the major hysteresis loop between -1 and 1 pu (in post inrush steady state). If this is done so fast as is partially the case in this figure in the negative flux direction, then the flux and current will build up faster than the transient exponential delay.

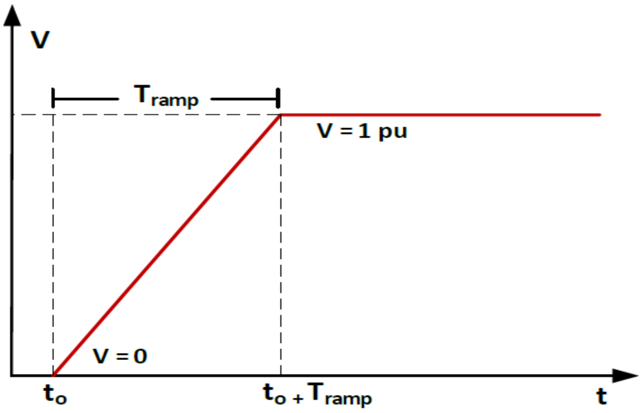

(a)

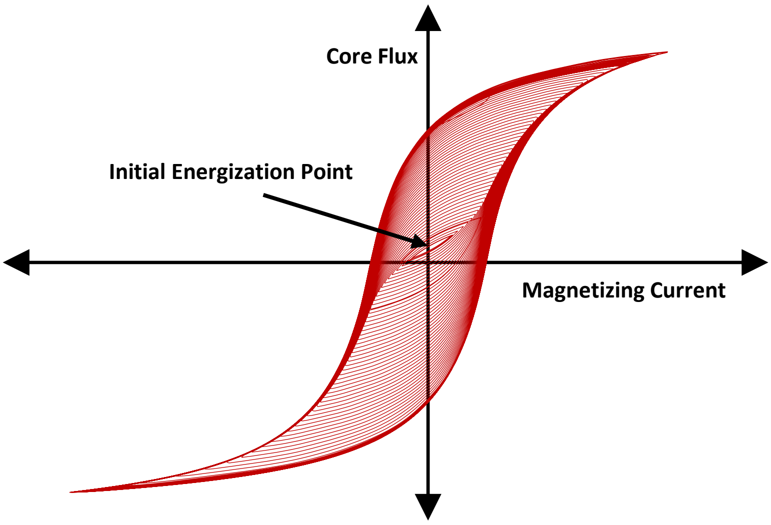

(b)

Figure 6: Soft transformer energization concept illustration: (a) voltage ramp example, (b) resulting magnetizing curve that spirals gradually starting from the initial starting point until approaching the major loop.

Consequently, optimizing the ramping time based on transformer parameters to avoid selecting short times that can lead to saturation becomes an important task. In contrast, even if residual flux ϕ_r measurement is not available, then the ramping time can be selected to consider the worst case ϕ_r scenario as a starting point, and then assigning T_{ramp} to be long enough such that the core does not go into deep saturation. Table 1 presents a high-level comparison between the four discussed transformer energization techniques. Finally, newer techniques presented in the literature aim to combine some of the main presented ones, such as combining the transformer core pre-fluxing or de-fluxing with controlled energization or fast ramps.

Table 1: High-level summary of different transformer energization techniques for inrush current mitigation.

	Principle of Operation	Required Measurements	Independent Breakers?	I_m Mitigation Effectiveness
Hard Energization	Simultaneous energization for all phases at a random instant	None	No	Low
Pre-Insertion Resistors	Same as previous but with series resistors to limit inrush current	None	No	Medium
Controlled Switching	Eliminating the effect of residual flux through point-on-wave switching	Flux and input voltage (including residual flux)	Yes	High
Soft Energization	Ramping the source voltage to slow the core saturation effect until transient decay	**Basic:** None **Optimized:** V, ϕ and transformer parameters with $\phi - i_M$ curve	No	**Basic:** Medium **Optimized:** High

3. Transformer Energization Simulations

Simulated tests for single and three phase transformer energizations are presented and discussed here to provide a deeper perspective on the implications of using each technique. The results for single phase transformers are first presented to study the energization impact on a single transformer core and demonstrate the operation of each technique without intra-phase operational interference. Notably, referring to equation (1), and its variations, in addition to the presented results: a description of the sensitivity impact of the different involved parameters is observed. The simulations are extended to three-phase transformers using different configurations such as wye and delta connected primary windings to understand the variations of their energization by the investigated techniques and form a more complete picture instead of relying on a single transformer type for the analysis.

3.1. Simulation Model Assumptions

In the presented MATLAB/Simulink based tests, the transformer models are energized through voltage sources without considering the possible voltage distortions arising from current control. The magnetizing current is set to minimal values for -1.1 to 1.1 pu flux range (curve knee value), with low air-core inductance. In practice, the knee value can be higher at around 1.1-1.3 pu. The lower end range is considered in this report to demonstrate simulations closer to worst-case scenarios.

A transformer core saturation curve (defined on the stricter saturation end) is thus used. The curve is defined in MATLAB/Simulink using the piecewise approximation with residual flux compatibility up to 0.85 pu. The adopted approximations and the numeric simulations nature are observed to cause some deviations that underestimate flux magnitudes when the transformer model goes into deep saturation. This is more evident at the case of hard energization simulations since the other techniques aim to avoid core saturation in first place. Collectively, the presented results maintain accurate inrush behavior trends between the different techniques: hard energization (high probability of large inrush current due to random switching), controlled energization (near elimination of inrush current) and soft energization (ramping time inrush current dependency). The presented peak flux and inrush currents in this report should not be considered as absolute numbers generalized to any transformer core or saturation case, but rather as indicators to study inrush current mitigation techniques and their capabilities.

The same piecewise linear saturation curve is used across all energization tests for single and three phase transformers in this report for consistency, and is illustrated in Figure 7. Table 2 summarizes the transformer parameters used uniformly for each test. The key differences between different cases are: single phase test transformer rating is $\frac{53}{3}$ MVA, and the base current and flux values for delta connected transformers are defined with respect to line-to-line voltages. Finally, residual flux values are defined and listed when describing each test.

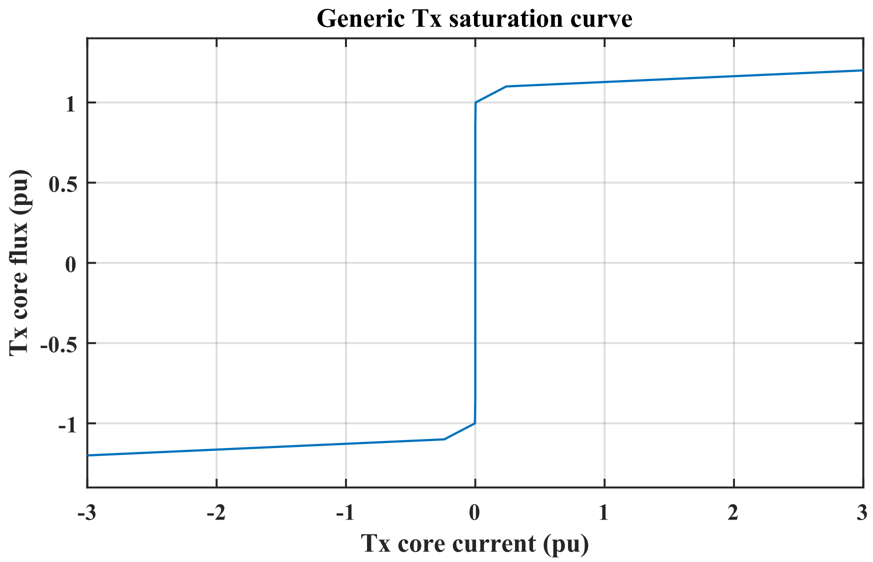

Figure 7: Core saturation curve used throughout the simulations in this report.

Table 2: Parameters used for transformers energization tests.

Parameter	Value	Parameter	Value
3P Rating (MVA)	53	**Windings Resistance (pu)**	0.002
Primary V_{LL} (kV)	11	**Windings Inductance (pu)**	0.08
Secondary V_{LL} (kV)	33	**Flux Path Return Inductance (pu)**	0.5 (for 3P single core only)
Core Resistance R_m (pu)	500	**Base Frequency (Hz)**	50

3.2. Single Phase Transformers

Hard Transformer Energization

In this test, the transformer is initially connected with the core flux and voltage operating under nominal conditions between -1 and 1 pu with consequently negligible magnetizing current. The results are illustrated in Figure 8. At t = 0.1 s, the transformer is disconnected, and a residual flux of 0.85 pu remains at the core. Then, at t = 0.2 s, the transformer is re-energized by the 1 pu voltage source. Residual flux impact is combined with the energization instance and the flux consequently jumps to a higher value than the saturation region limit, triggering a significant inrush current that approaches 6 pu. This magnitude is influenced by the modeling assumptions highlighted in section 3.1 and the saturation curve defined in Figure 7. Evidently, varying the energization angle α directly impacts the inrush current magnitude in this case. Energizing the transformer at another random instant would have resulted in a different inrush current magnitude (higher or lower). This randomness serves to illustrate the key limitation of relying on this technique.

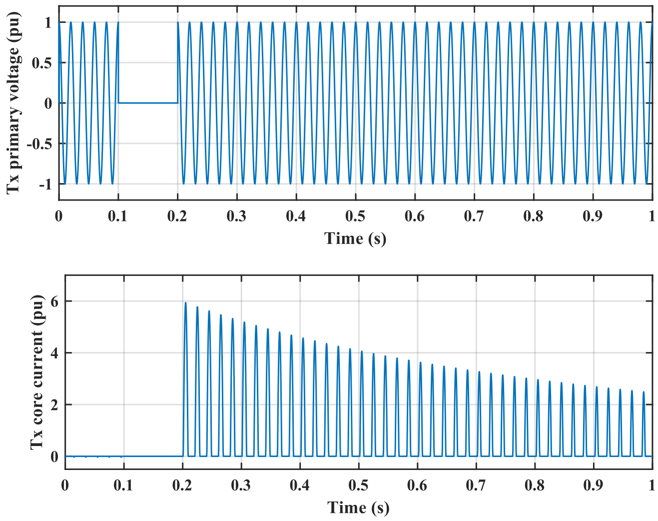

Figure 8: Hard transformer energization for a single-phase core.

Hard Transformer Energization with Pre-Insertion Resistor

On the other hand, energizing the transformer under the same conditions but with higher energizing side series resistance results in: a) lower inrush current magnitude due to lower flux jump, b) faster inrush current decay due to the higher system damping. The example presented in Figure 9 illustrates this behavior using an energizing side resistance that is tens of times higher than the one presented in Figure 8, with the same energization angle as before. Connecting higher resistances in series can reduce the magnetizing current peak below 1 pu, at the expense of higher losses. Practically, several techniques to limit this additional loss to the energization instant are proposed in the literature, such as circuit re-routing at steady state or the use of thermal resistors as described earlier in section 2.

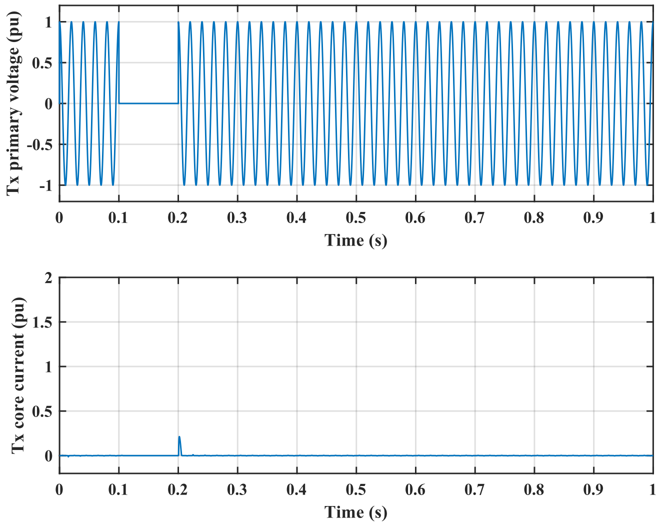

Figure 9: Hard transformer energization with higher energizing side resistance (pre-insertion resistor).

Controlled Transformer Energization

In this test, the same sequence as before is adopted, the transformer is de-energized at t = 0.1 s, the residual flux is at 0.85 pu, and the re-energization signal is received at t = 0.2 s. However, in this case, the breaker does not immediately close as before. Instead, the prospective flux is monitored, and the breaker is only closed once the residual and prospective flux are equal (a tolerance range of 0.05 pu is introduced in the simulations to account for discrete sampling impact as matching values are difficult to achieve through the analog to digital converters in practice, or discrete simulations in software). Figure 10 illustrates the result, showing the transformer re-energization-controlled sequence. The inrush current is almost null, and the flux moves along its prospective value after energization.

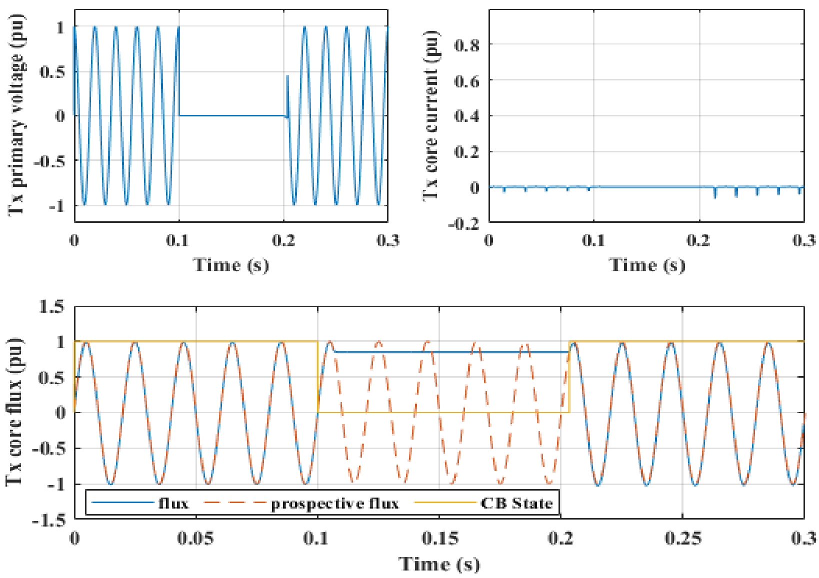

Figure 10: Controlled (point-on-wave) energization of a single-phase transformer.

Soft Transformer Energization

Energizing a transformer through a ramping voltage does not necessarily eliminate inrush current. A mis-selection of the ramping time (too fast) can still lead to delayed, but inevitable, large inrush current. The definition of too fast is dependent on the specific used transformer model parameters, as well as the residual flux at the energizing moment. For the simulated model with a residual flux of 0.85 pu, re-energizing the transformer in 1 second results in a reduced inrush peak (around 4 pu compared to 6 pu previously). The results for this test are summarized in Figure 11.

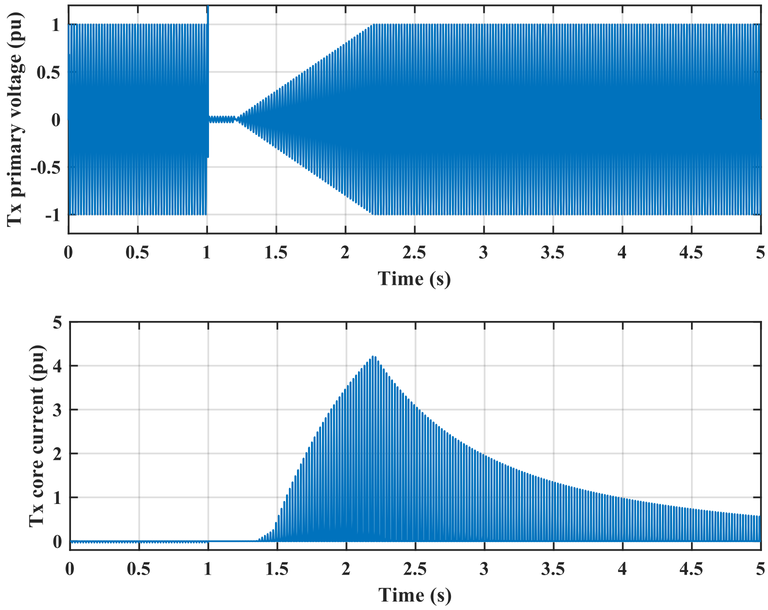

Figure 11: Soft transformer energization with Tramp = 1 second.

For this scenario, increasing the ramping time to 10 seconds with the same parameters did not mitigate the inrush current issue to a value below 1 pu value due to flux saturation (see Figure 12a). In comparison, if the transformer parameters and ramping time are maintained, and only the primary winding resistance is tripled, then $T_{ramp} = 10\, seconds$ is effectively sufficient (see Figure 12b). Several ramping times are reported in literature by manufacturers and researchers. The range found in these reports can be up to tens of seconds, depending on the system complexity, initial conditions, connected network impedance and the number of energized transformers.

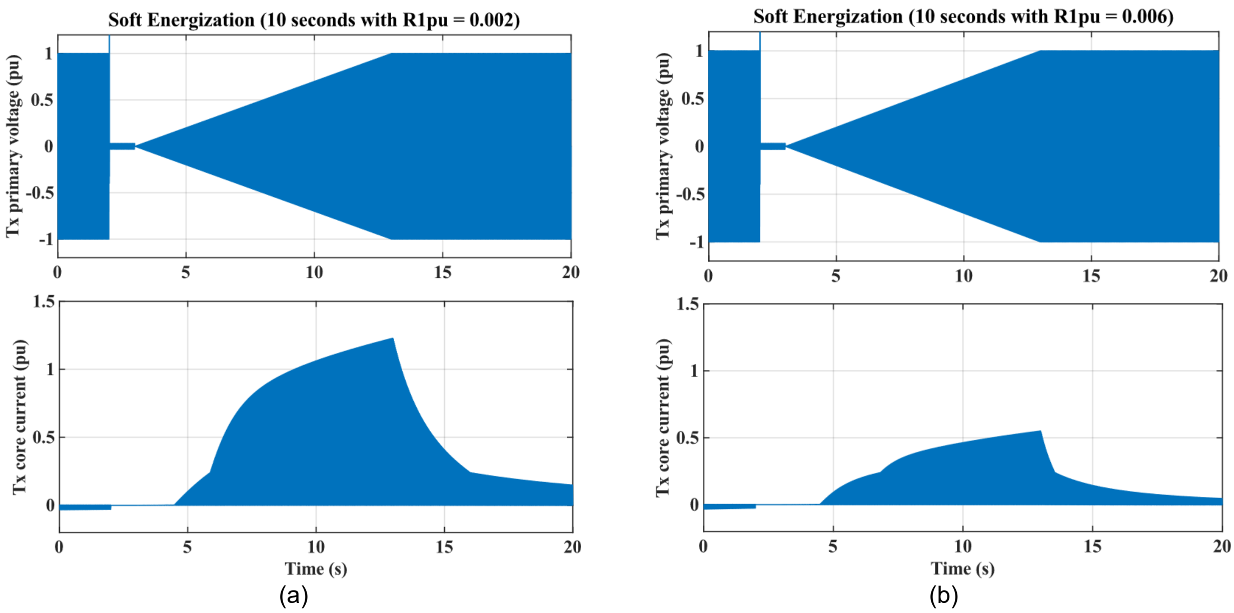

Figure 12: Soft transformer energization with Tramp = 10 seconds: (a) R1pu = 0.002 pu, (b) R1pu = 0.006 pu.

3.3. Three Phase Transformers

The extension of single-phase transformer energization tests to various three phase configurations is summarized in this subsection, highlighting key differences and special requirements. The covered techniques are similarly hard, controlled, and soft energization. The considered configurations cover both delta and wye connected primary windings. The secondary sides are all connected in wye-grounded configurations. The impact of secondary side configuration is briefly described in the controlled energization subsection.

Hard Transformer Energization

This test is performed on delta and wye connected primary transformers. Here, the transformers are initially operated normally, disconnected at t = 3 s, and reconnected at t = 3.1 s. The presented results are based on the same parameters as in Table 2, and are shown in Figure 13a for delta primary transformer, and Figure 13b for wye primary transformer. In Figure 13a, the source phase voltages are shifted by 30 degrees when applied to the primary delta windings as the core voltages are line-to-line. Hence, the inrush current between Figure 13a and Figure 13b is noticeably different. These plots thus illustrate the extreme extent to which the inrush current magnitude is impacted by the energization instant. In other words and given the independent phases and cores nature for the transformer model used in Figure 13b (wye connection), it can be considered as three independent transformers being energized with 120 degrees phase shift. The inrush magnitude variations are very significant, although phase A current peaked around 0.45 pu, phase B inrush current peak was around 10 pu, based on the used common saturation curve in Figure 7.

Controlled Transformer Energization

Requirements for controlled three phase transformer energization vary based on the transformer configuration. In this subsection, the tests presented aim to illustrate some of these variations by covering different primary winding connections. Here, the considered secondary connection is maintained as grounded wye to have a neutral impact on the energization procedure, whereas in practice having a delta secondary can impact the energizing side in some cases (e.g., for a wye-delta transformer).

A key difference between energizing three core wye and delta windings in this test is that the wye primary is phase independent in the sense that if one phase breaker is energized then a voltage would form between the corresponding phase winding and the ground (see Figure 14a), whereas two phase breakers are required to energize the line-to-line voltage in case of delta primary connection, and the other two transformer phases will be partially energized to equalize the delta voltage loop (i.e., generating a voltage that adds up to equalize the voltage formed on the first energized phase as in Figure 14b).

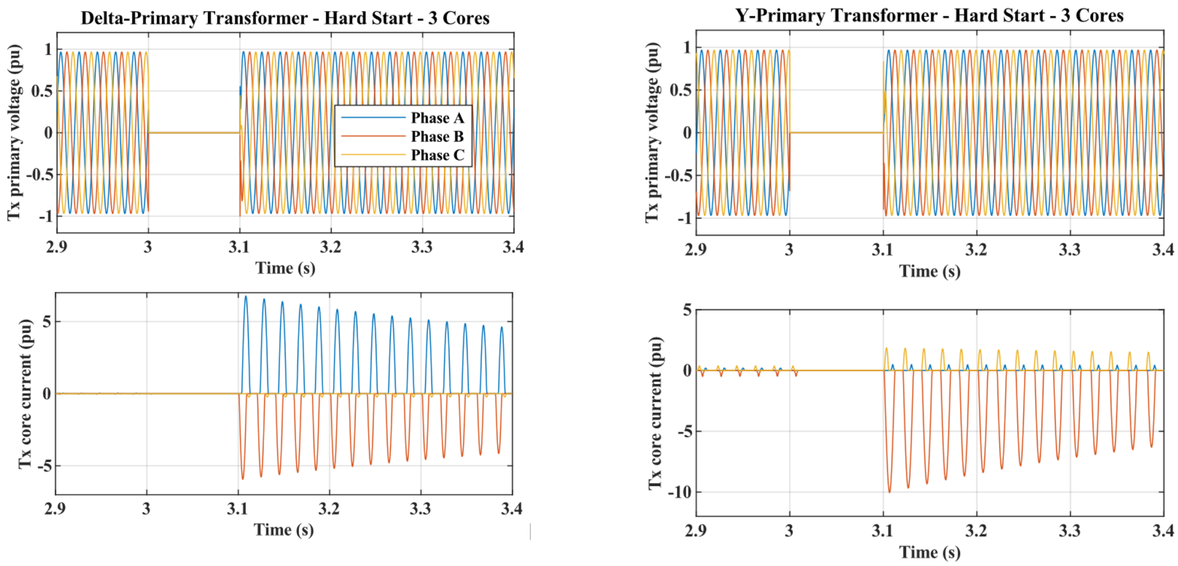

(a) (b)

Figure 13: Three phase hard energization simulation results: (a) three cores delta-wye transformer, (b) three cores wye-wye transformer.

These voltages can correspondingly impact the core flux and breakers closing sequence. That is, the three cores wye-wye transformer in Figure 14a may be treated as three individual replicas to the closing sequence in the single-phase transformer (Figure 10). Whereas the delta primary transformer differs in that two phase breakers are simultaneously energized based on their line-to-line prospective

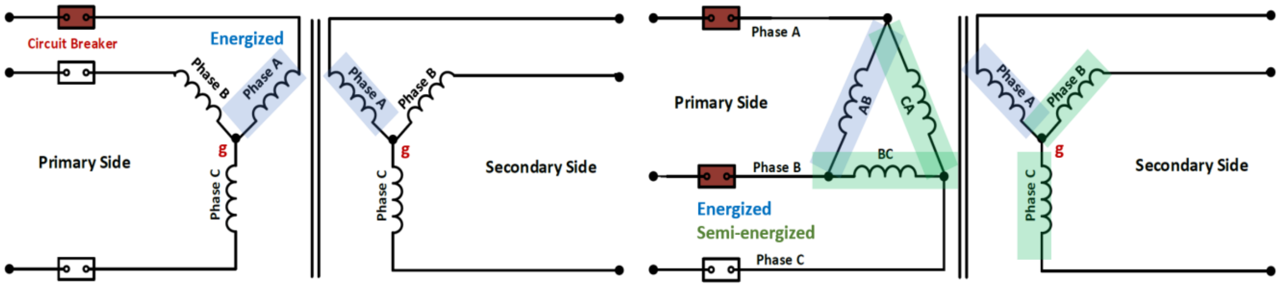

(a) (b)

Figure 14: Configuration-based variation in controlled transformer energization sequence: (a) three cores wye-wye transformer, (b) three cores delta-wye transformer, red indicates closed breaker.

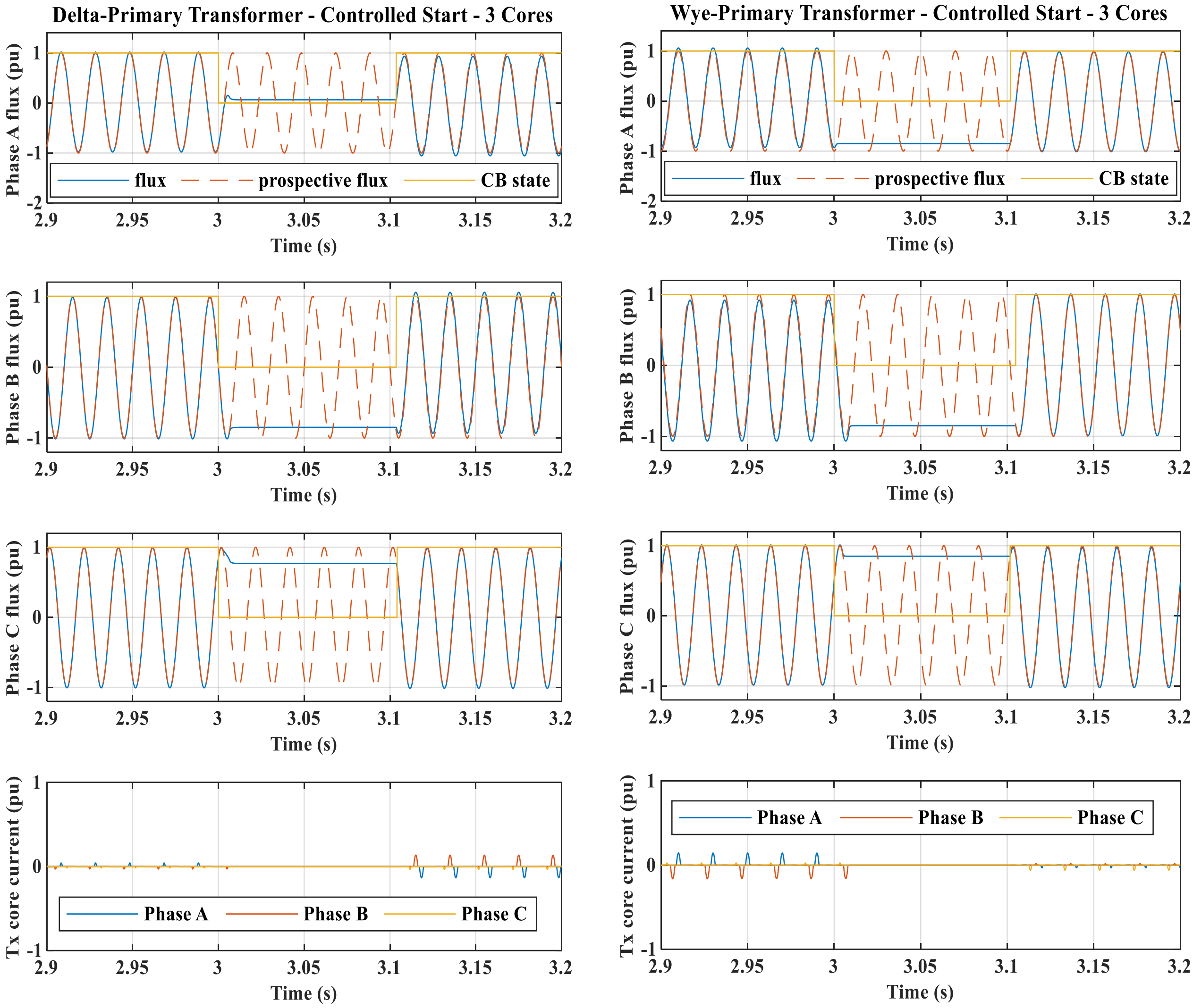

(a) (b)

Figure 15: Three-phase controlled energization simulation results: (a) three cores delta-wye transformer, (b) three cores wye-wye transformer.

flux to satisfy the controlled switching requirement (e.g., phases a and b), and then the third phase breaker is closed when the rest of the requirements are achieved. This is illustrated in Figure 15a, where the transformer phase flux waveforms are generated through line-to-line source voltage integrations rather than phase voltages. Here, breakers a and b are simultaneously closed, and breaker c follows shortly after. On the other hand, Figure 15b shows the results for the wye primary transformer, with the three phases closing independently.

Soft Transformer Energization

For this test, similar ramping periods to those applied on single-phase transformers are used on a three-core delta connected primary transformer. The transformer is also initially connected under normal operating conditions, disconnected at t = 3 s and then reconnected at t = 3.1 s. All phases are energized simultaneously here, so the variations discussed in controlled start case are not expected to have similar impact, provided that sufficient ramping time is used.

The residual fluxes are system generated in this case based on the disconnection instant and range between -0.85 and 0.85 per unit according to the used saturation curve in the simulations. The results are summarized in Figure 16. For a one second ramp, the inrush current magnitudes for phase B and C are considerably high due to their large pre-energization residual fluxes, whereas phase A maintains a near-zero inrush current ($\phi_{RA} = 0.07\,pu, \phi_{RB} = -0.85\,pu, \phi_{RC} = 0.78\,pu$).

A ramp of 10 seconds was also applied to the same transformer and the resulting inrush magnitudes in phase B and C were close to those reported in single phase case for $R_{1pu} = 0.002\,pu$ in Figure 12, reduced below 1 pu.

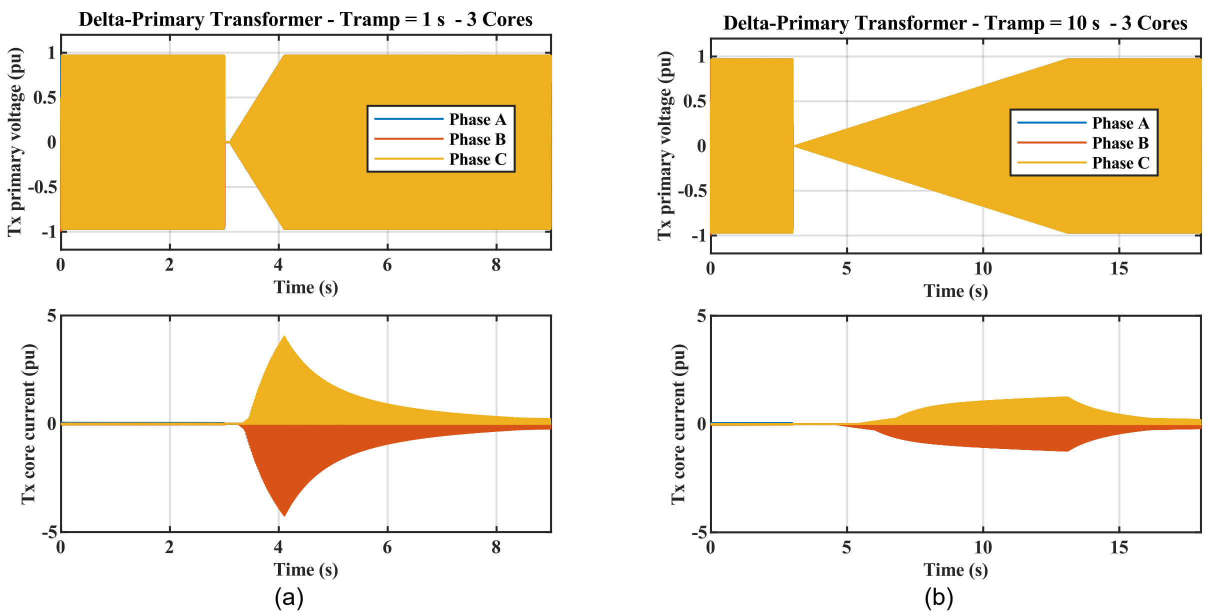

Figure 16: Soft energization of a three-phase transformer (delta-wye, 3 cores): (a) Tramp = 1 s, (b) Tramp = 10 s.

4. Grid-Forming Converter Control for Black-Start

The first deliverable of this study included a comparison between four grid forming converters control techniques. Each of these techniques (droop, power synchronizing control (PSC), virtual synchronous machine (VSM) and matching control) showed satisfactory performance against a wide range of disturbances and operating conditions such as active power, DC voltage and load disturbances in addition to ramping voltage reference tracking. In this report, extended analysis and simulations are carried out using the VSM control. This controller is selected due to its wide range of capabilities, including inertia emulation and fast frequency response.

In this report, the classical VSM structure is slightly modified to achieve the requirements of a complete black-start scenario based on the network presented in Figure 1. The VSM is also connected to inner current control loops for protection (see Figure 17). The outer voltage loop sets the reference current values to the inner current loop based on the operation set-point and ensures that both direct and quadrature reference currents are maintained within the converter operating limits. The cross-coupling terms $\omega_{ref}C_f$ & $\omega_{ref}L_1$ are imposed to decouple both axes operation, and the feedforward terms enabled by FF1 and FF2 are typically added to improve and the control performance and disturbance rejection. Finally, the controlled current loop output is reverted to the abc frame to generate the Pulse-Width-Modulation (PWM) driving signals to the grid forming converter switches.

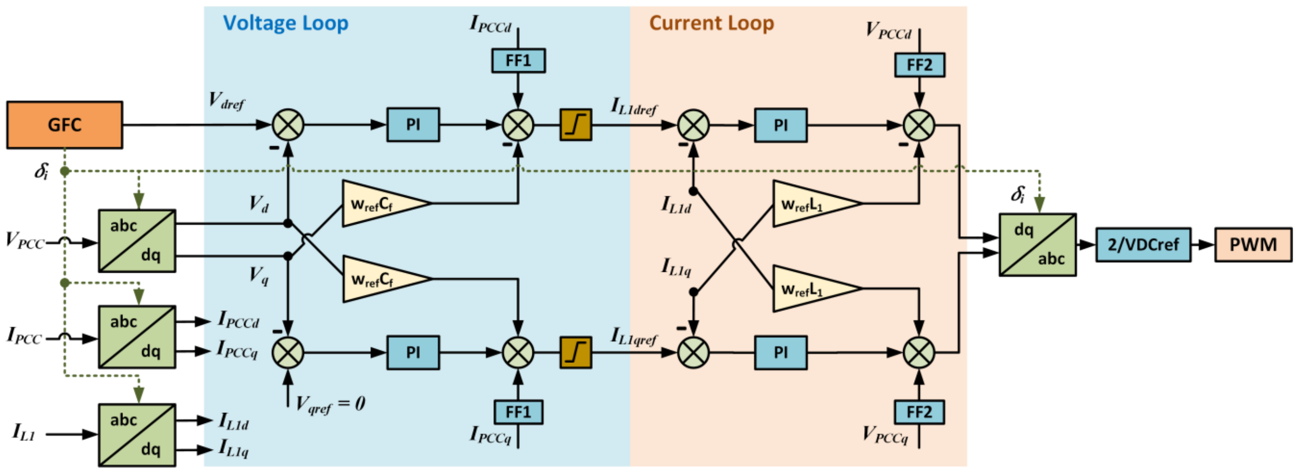

Figure 17: Inner voltage and current control loop interfaced to GFC control output.

The target scenario presented in this section includes three main steps that are carried out in sequence. First, transformer energization through soft energization. Second, load pickup is performed at the point-of-common coupling (PCC). Third and last, grid synchronization through modifying the VSM control angle to match that of the grid after receiving a grid-connection signal from the utility. These steps are summarized in Figure 18.

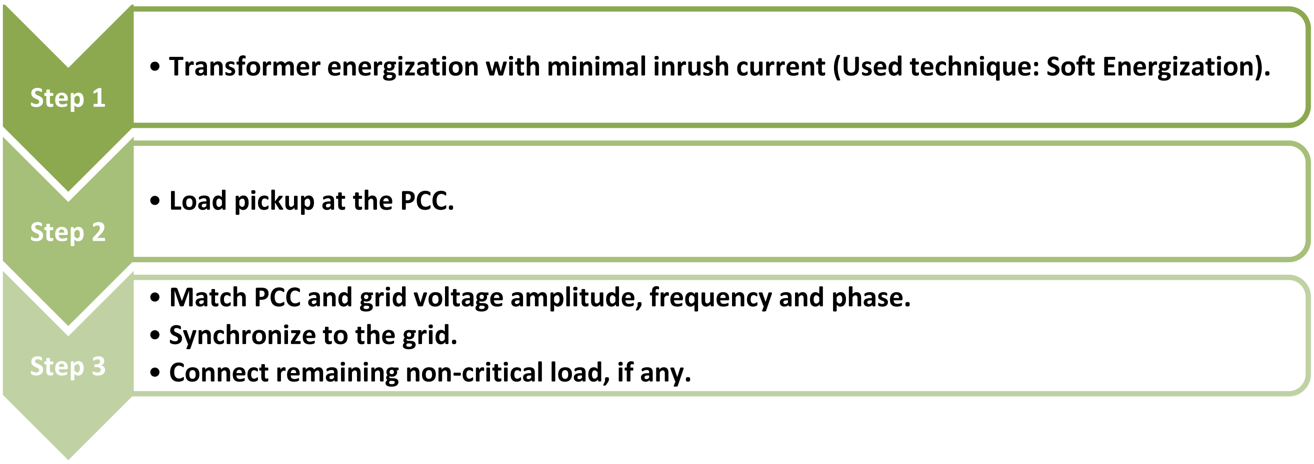

Figure 18: GFC based simulated black-start scenario steps.

The covered cases investigate the connection of full load at the PCC instantly and the impact of that on the PCC voltage, versus the gradual connection of separate load blocks before and after grid connection. Unified system parameters were used across the test scenarios. The VSM power loop is designed to produce 0.25 Hz error at full power reference mismatch. The used transformer topology is single core three phase $\Delta - \Delta$ configuration with a similar saturation curve to that used in Section 3. The transformer is rated at 53 MVA, based on that of a distribution transformer in Chaplecross network, Scotland. The combined system parameters are summarized in Table 3.

Table 3: Simulated network parameters for the GFC black-start tests.

Parameter	Value	Parameter	Value
Converter Rating (MVA)	40	**P and Q Reference (MW, MVAR)**	35, 5
$\Delta - \Delta$ Transformer Rating (MVA)	53	**System Frequency (Hz)**	50
Converter Output Voltage (kV_{LL})	11	**Filter & Grid X/R Ratio**	10
Grid Voltage (kV_{LL})	33	**Grid Short-Circuit-Ratio (SCR)**	5

4.1. Modified VSM Control

The modified VSM controller block diagram is presented in Figure 19. The main adjustments are related to voltage control and synchronizing capabilities. VSM voltage reference is modified to a saturated ramp at steady-state voltage to accommodate soft transformer energization requirements. After transformer energization and load pickup are achieved, smooth grid synchronization requires the matching of voltage signals at the PCC from both the grid and the energized island sides in terms of magnitude, frequency, and phase.

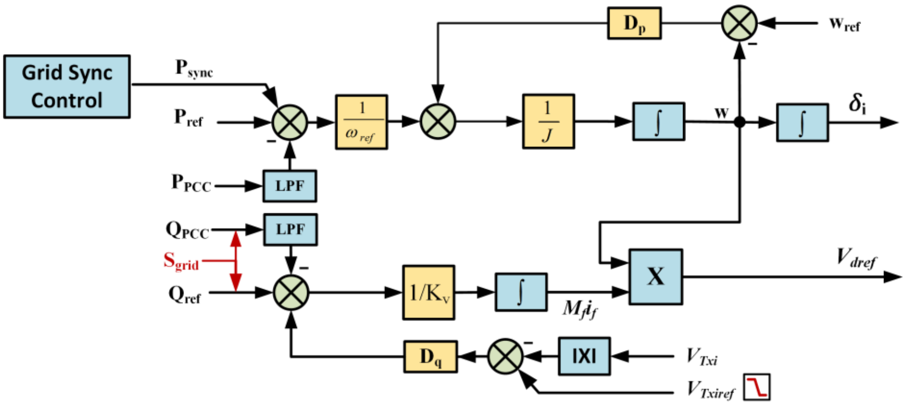

Figure 19: Modified VSM control for transformer energization and black-start.

The voltage magnitudes are matched through setting the PCC voltage reference to that of the grid voltage (with the aid of voltage drop compensators such as transformer OLTC or an optional integrated VSM compensator in the voltage loop).

Smooth synchronizing to the grid can be achieved by fine-tuning the VSM output to influence that at the PCC such that it matches the grid voltage phase. This grid angle matching control in Figure 19 can be realized by means of PI control. The synchronization action should consider the converter power reference to mitigate active and reactive power jumps at the synchronization instant. Once synchronization is achieved, the converter active and reactive power references are followed to export/import power with the grid as dictated by the application requirements.

Figure 20 illustrates a generic example for grid disconnection and restoration to visualize the gradual phase matching action, where DS refers to an island distribution system. In island operation after t = 0.05, an artificial 90 degrees shift is induced prior to activating the re-synchronizing PI controller to demonstrate the smooth control action.

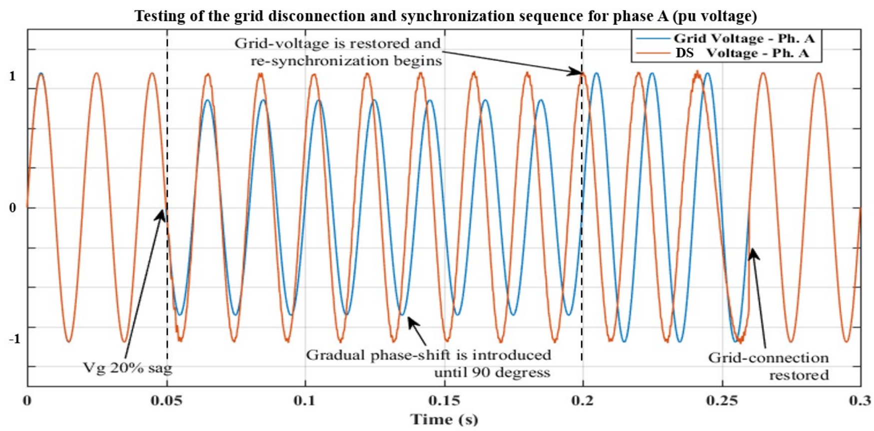

Figure 20: Generic grid disconnection/re-synchronization sequence.

4.2. Simulated Black-Start Scenarios

The presented simulation results here follow the sequence presented in Figure 18 for a balanced three-phase system. Starting with transformer energization using soft energization, followed by block load pickup and grid synchronization. The covered scenarios are summarized as below:

1) Full-Load pickup at the PCC followed by grid synchronization.
2) Sequential pickup of 50% load at the PCC followed by grid synchronization and connection of the remaining 50% load.

Residual flux for all three tests is defined as $\phi_{RA} = -0.85\ pu, \phi_{RB} = 0.6\ and\ \phi_{RC} = 0.25$. It has been observed that the inrush current mitigation through soft energization can be faster when integrated to converters current control due to the added current limits. Though, such integration should be approached carefully to limit severe violations of the converter behavior as a voltage source.

Scenario 1: Full Balanced Load Pickup

In this test, the ramping time is set to $T_{ramp} = 10\ s$. The ramping reference between 0 and 1 pu is supplied to the VSM control voltage loop in Figure 19 and is tracked to produce the transformer energizing voltage by the converter. As observed in Figure 21, the flux is maintained below 1.1 pu in all phases and the magnetizing inrush current is consequently minimal.

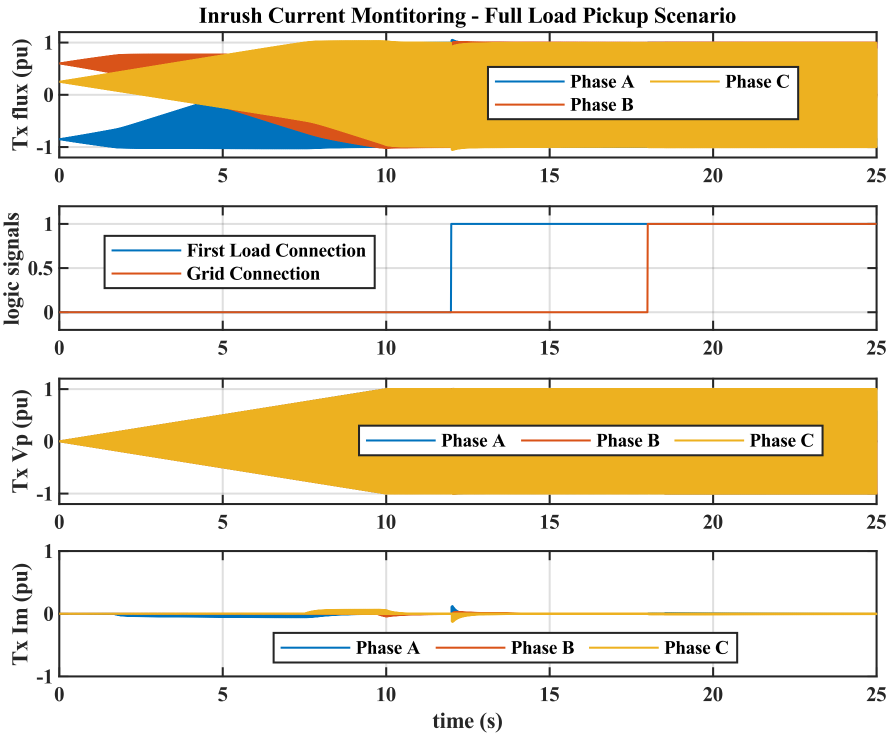

Figure 21: VSM transformer energization with full balanced load pickup: inrush current monitoring.

Once the transformer is fully energized at t = 10 s, a one second delay is induced, followed by full load block connection at the same instant around t = 12 s (35 MW). This leads to momentary decrease in voltage that is compensated by additional VSM reactive power injection. Then, grid synchronization sequence is initiated, and the PCC switch is closed around t = 18 s for grid connection.

During transformer energization, the power consumption is negligible due to the inrush current mitigation strategy. The converter output frequency trace remains mostly within limits. These results are summarized in Figure 22. Initially, frequency maintains a value around 50.22 Hz during transformer energization due to the near zero active power consumption and the generated VSM power loop error. Then, a peak of 50.41 Hz is generated at the instant of load connection before settling down around 50 Hz. During synchronization, the frequency follows the behavior of the power synchronization controller and settles back at 50 Hz once voltage angles between the PCC and the grid are matched.

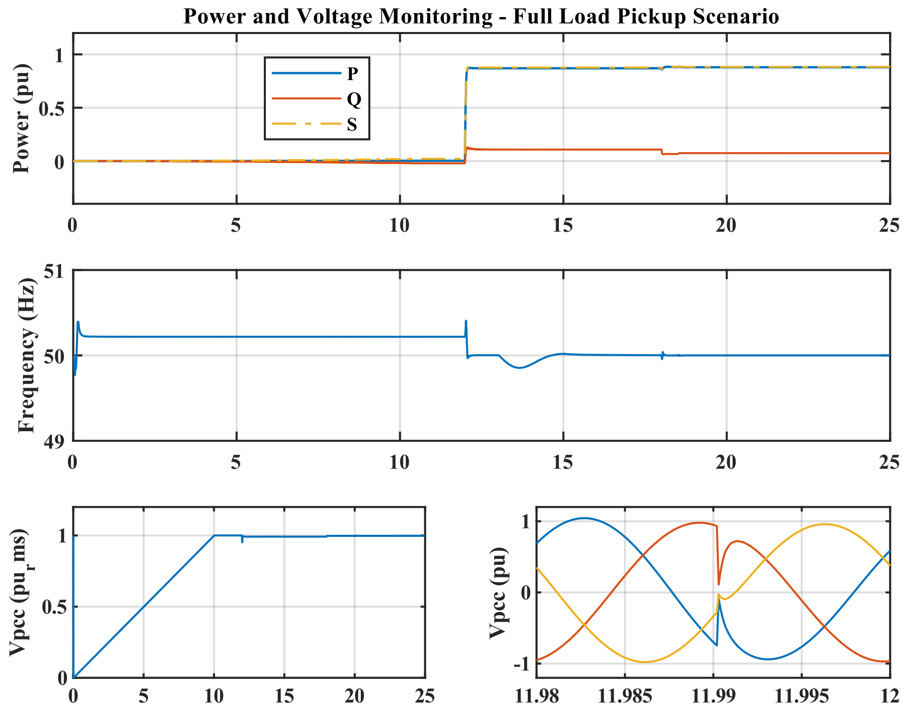

Figure 22: VSM black-start with full balanced load pickup: power, voltage and frequency monitoring.

Scenario 2: Sequential Load Pickup

The transformer energization and inrush current patterns for this test are similar to the full load pickup case, and thus the results are not presented here again. Instead, we focus on the power, frequency and voltage traces. In this scenario, the load is sequentially connected in smaller blocks to visualize the system parameters variation as compared to full instantaneous load pickup. The load connection sequence is illustrated in Figure 23 (100% indicates 35 MW load connection). Where 50% of the load considered critical during black-start, and the remaining 50% are connected after grid synchronization.

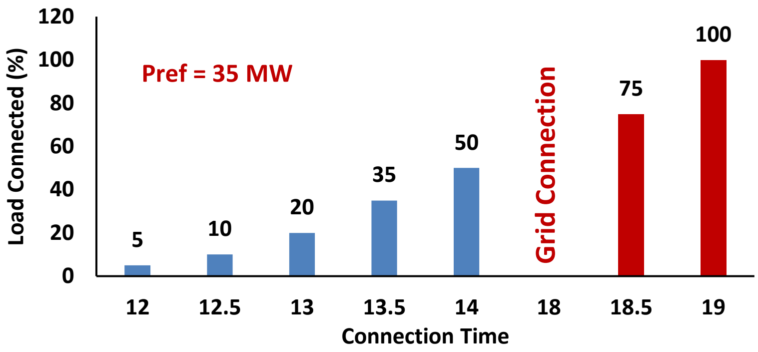

Figure 23: Load connection sequence for the sequential load pickup scenario.

The results are illustrated in Figure 24. Similar to the previous case, the transformer is energized without violating inrush current requirements, and the first load block (5%) is then connected at t = 12 s. The rest of the load is connected following the defined sequence. Clearly, the process is smoother and the time-domain voltage disturbance to the sinusoid voltages are significantly reduced. The f-trace disturbances are of lower magnitudes, and the grid connection at t = 18 s results in a smooth transition and settling of the converter frequency to 50 Hz.

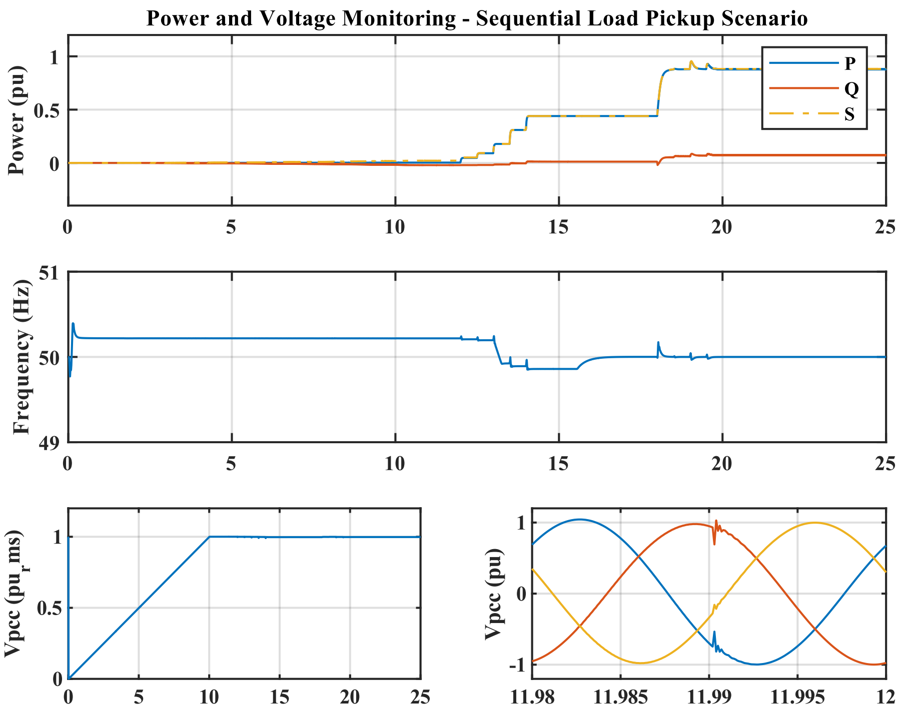

Figure 24: VSM black-start with sequential balanced load pickup: and voltage monitoring.

Collectively, the full and sequential connection scenarios present two extreme cases to highlight the response variations and assist in understanding the impact of various load connection cases on the variability of VSM control performance. It is noteworthy that the transformer parameters (and the impedance between the inverter and the PCC) contribute to the variation of voltage drop magnitudes.

5. Remarks

Black-start from non-conventional generation, especially using converters-based resources, is picking industrial pace as an important ancillary service to be provided by DERs amidst their accelerated replacement of synchronous generators. This report covered two main relevant points, namely transformer energization as part of black-start sequence, and a modified VSM that is capable of participating in black-start through transformer energization, load pickup and grid synchronization.

Simulations of hard, controlled, and soft transformer energization techniques are presented to benchmark their capabilities using voltage source energization. It is demonstrated that transformer model, network impedance, core saturation characteristics, energization instant and residual flux are amongst the key parameters influencing inrush current across hard and controlled energization techniques, in addition to the ramp time for soft energization. The implementation of controlled transformer energization requires the existence of independent phase breakers that can be controlled individually in a timely manner, whereas soft energization does not require this functionality.

The modified VSM is equipped with soft energization and grid synchronization capabilities. The full converter-transformer-load-grid system was tested using soft transformer energization, and a successful black-start sequence of the considered system was achieved with minimal inrush current. Practical implementation of the presented synchronizing controller requires the existence of reliable communication links between the converter control unit and the PCC, to feedback the VSM controller with grid and PCC voltages to match their voltage angles.

6. Bibliography

[1] S. Fang, H. Ni, H. Lin, and S. L. Ho, "A Novel Strategy for Reducing Inrush Current of Three-Phase Transformer Considering Residual Flux," *IEEE Transactions on Industrial Electronics,* vol. 63, no. 7, pp. 4442-4451, 2016.

[2] R. Cano-González, A. Bachiller-Soler, J. A. Rosendo-Macías, and G. Álvarez-Cordero, "Controlled switching strategies for transformer inrush current reduction: A comparative study," *Electric Power Systems Research,* vol. 145, pp. 12-18, 2017.

[3] H. Ni, S. Fang, and H. Lin, "A Simplified Phase-Controlled Switching Strategy for Inrush Current Reduction," *IEEE Transactions on Power Delivery,* vol. 36, no. 1, pp. 215-222, 2021.

[4] J. Mitra, X. Xu, and M. Benidris, "Reduction of Three-Phase Transformer Inrush Currents Using Controlled Switching," *IEEE Transactions on Industry Applications,* vol. 56, no. 1, pp. 890-897, 2020.

[5] J. H. Brunke and K. J. Frohlich, "Elimination of transformer inrush currents by controlled switching. II. Application and performance considerations," *IEEE Transactions on Power Delivery,* vol. 16, no. 2, pp. 281-285, 2001.

[6] J. H. Brunke and K. J. Frohlich, "Elimination of transformer inrush currents by controlled switching. I. Theoretical considerations," *IEEE Transactions on Power Delivery,* vol. 16, no. 2, pp. 276-280.

[7] Z. Taghikhani, M. A. Taghikhani, and G. B. Gharehpetian, "Inrush current modeling of three-limb core-type power transformers based on efficient analytical-numerical hybrid method," *International Journal of Electrical Power & Energy Systems,* vol. 117, p. 105694, 2020/05/01/ 2020.

[8] P. Pachore, Y. Gupta, S. Anand, S. Sarkar, P. Mathur, and P. K. Singh, "Flux Error Function Based Controlled Switching Method for Minimizing Inrush Current in 3-Phase Transformer," *IEEE Transactions on Power Delivery,* pp. 1-1, 2020.

[9] R. Oyanagi, T. Noda, and M. Ichikawa, "A Method for Estimating the Current–Flux Curve of a Single-Phase Transformer for Electromagnetic Transient Simulations of Inrush Currents," *Electrical Engineering in Japan,* vol. 204, no. 2, pp. 13-24, 2018,

[10] K. A. Bhatt, B. R. Bhalja, and U. B. Parikh, "Evaluation of controlled energisation of an unloaded power transformer for minimising the level of inrush current and transient voltage distortion using PIR-CBs," *IET Generation, Transmission & Distribution,* vol. 12, no. 11, pp. 2788-2798, 2018.

[11] U. Parikh and B. R. Bhalja, "Mitigation of magnetic inrush current during controlled energization of coupled un-loaded power transformers in presence of residual flux without load side voltage measurements," *International Journal of Electrical Power & Energy Systems,* vol. 76, pp. 156-164, 2016.

[12] C. Yu, S. G. Abdulsalam, C. Shiuming, and X. Wilsun, "A sequential phase energization technique for transformer inrush current reduction - Part I: Simulation and experimental results," *IEEE Transactions on Power Delivery,* vol. 20, no. 2, pp. 943-949, 2005.

[13] X. Wilsun, S. Abdulsalam, C. Yu, and L. Xian, "A sequential phase energization technique for transformer inrush current reduction part II: theoretical analysis and design guide," in *IEEE Power Engineering Society General Meeting, 2004*, p. 534 Vol.1, 2004.

[14] A. Peña Asensio, F. Gonzalez-Longatt, S. Arnaltes, and J. L. Rodríguez-Amenedo, "Analysis of the Converter Synchronizing Method for the Contribution of Battery Energy Storage Systems to Inertia Emulation," *Energies,* vol. 13, no. 6, 2020.

[15] J. Wang, A. Pratt, and M. Baggu, "Integrated Synchronization Control of Grid-Forming Inverters for Smooth Microgrid Transition," in *2019 IEEE Power & Energy Society General Meeting (PESGM)*, pp. 1-5, 2019.

[16] J. Wang, B. Lundstrom, and A. Bernstein, "Design of a Non-PLL Grid-forming Inverter for Smooth Microgrid Transition Operation," in *2020 IEEE Power & Energy Society General Meeting (PESGM)*, pp. 1-5, 2020

[17] J. E. Holcomb, "Distribution Transformer Magnetizing Inrush Current," *Transactions of the American Institute of Electrical Engineers. Part III: Power Apparatus and Systems,* vol. 80, no. 3, pp. 697-702, 1961.

[18] C. G. A. Koreman, "Determination of the magnetizing characteristic of three-phase transformers in field tests," *IEEE Transactions on Power Delivery,* vol. 4, no. 3, pp. 1779-1785, 1989.

[19] S. McGuinness *et al.*, "Coordination of AC protection settings during energisation of AC grid from a VSC HVDC interconnector," *IET Conference Proceedings,* pp. 6 pp.-6 pp.

[20] C. P. J. Jansen, J. G. Slootweg, and R. A. C. T. d. Groot, "Calculation of Transformer Inrush Currents occurring during the Energizing of the Public Grid after a major Black Out," in *2005 IEEE Russia Power Tech*, pp. 1-7, 2005.

[21] S. G. Abdulsalam, X. Wilsun, W. L. A. Neves, and L. Xian, "Estimation of transformer saturation characteristics from inrush current waveforms," *IEEE Transactions on Power Delivery,* vol. 21, no. 1, pp. 170-177, 2006.

[22] N. Chiesa, B. A. Mork, and H. K. Høidalen, "Transformer Model for Inrush Current Calculations: Simulations, Measurements and Sensitivity Analysis," *IEEE Transactions on Power Delivery,* vol. 25, no. 4, pp. 2599-2608, 2010.

[23] H. Jain, G. S. Seo, E. Lockhart, V. Gevorgian, and B. Kroposki, "Blackstart of Power Grids with Inverter-Based Resources," in *2020 IEEE Power & Energy Society General Meeting (PESGM)*, pp. 1-5, 2020.

[24] M. Aten, R. Shanahan, F. Mosallat, and S. Wijesinghe, "Dynamic Simulations of a Black Starting Offshore Wind Farm Using Grid Forming Converters," presented at the 18th Wind Integration Workshop, Dublin, 2019.

[25] Y. Pan, X. Yin, Z. Zhang, B. Liu, M. Wang, and X. Yin, "Three-Phase Transformer Inrush Current Reduction Strategy Based on Prefluxing and Controlled Switching," *IEEE Access,* vol. 9, pp. 38961-38978, 2021.